Chemical Science

ROYAL SOCIETY OF CHEMISTRY

EDGE ARTICLE

View Article Online
View Journal | View Issue

Check for updates

Cite this: *Chem. Sci.*, 2025, **16**, 5573

All publication charges for this article have been paid for by the Royal Society of Chemistry

Received 22nd January 2025
Accepted 19th February 2025

DOI: 10.1039/d5sc00589b

rsc.li/chemical-science

Ultra-high molecular weight polymer synthesis *via* aqueous dispersion polymerization†

Cabell B. Eades, Kaden C. Stevens, Danyella E. Cabrera, Micayla K. Vereb, Megan E. Lott, Jared I. Bowman and Brent S. Sumerlin *

The synthesis of ultra-high molecular weight (UHMW, $M_n \geq 10^6$ g mol^{-1}) polymers is generally complicated by the high viscosity of the resulting polymer solution. We report the synthesis of UHMW double-hydrophilic block copolymers (DHBCs) by leveraging polymerization-induced self-assembly (PISA) to obtain concentrated but free-flowing dispersions of UHMW water-soluble particles. By polymerizing *N*-acryloylmorpholine (NAM) from a poly(*N*,*N*-dimethylacrylamide) (PDMA) macroiniferter in the presence of a kosmotropic salt ($(NH_4)_2SO_4$), the salt sensitivity of the resultant poly(NAM) (PNAM) block induced self-assembly to result in free-flowing dispersions of polymeric particles (η < 6 Pa·s), despite the UHMW and high concentration of the newly formed block copolymer. To retrieve the UHMW polymer products, simple dilution with water lowered the $(NH_4)_2SO_4$ concentration sufficiently to resolubilize the PNAM chains, affording a highly viscous solution of fully dissolved DHBCs. The simplicity of this synthetic route has important implications for the facile production of UHMW materials on an industrial scale.

Introduction

Ultra-high molecular weight (UHMW) polymers ($M_n \geq 10^6$ g mol^{-1}) synthesized *via* reversible-deactivation radical polymerization (RDRP) techniques have recently become potentially important components in the development of next-generation materials.[1–4] While polymers in this molecular weight regime are accessible through a select group of conventional polymerization approaches, these methods generally do not allow access to materials with targetable molecular weights, functionalized chain ends, narrow molecular weight distributions, or advanced polymer architectures.[5,6] While RDRP techniques have been used to synthesize polymer materials bearing all these characteristics, achieving UHMW has traditionally proven challenging, requiring specialized reaction conditions, such as high pressures[7–9] or catalyst loadings.[10–13] Recent reports, however, have used more mild, accessible conditions to obtain UHMW materials.[4,14–19]

Notably, our group has demonstrated that photoiniferter polymerization can be leveraged to access UHMW polymers with excellent control over chain length and dispersity.[20–26] Hartlieb and coworkers have shown that the chain-end fidelity maintained during photoiniferter polymerizations can be exploited to permit the synthesis of block copolymers with 20 blocks and molecular weights exceeding 1800 kg mol^{-1}.[27] Despite the molecular weight range afforded by this photochemical approach, the synthesis of UHMW polymers ultimately yields viscous solutions that complicate purification and processing of the polymer product. In an attempt to remedy this issue, our research group has reported the synthesis of UHMW polymers in inverse miniemulsion conditions.[28–30] This heterogeneous approach maintains low solution viscosity by confining the polymerization to water droplets dispersed in a nonpolar solvent. Despite the success of this technique for low-viscosity UHMW polymer synthesis, the large amount of surfactant necessary to stabilize the reaction droplets may preclude its application on an industrial scale.

Polymerization-induced self-assembly (PISA) is another well-reported, heterogeneous methodology that leverages *in situ* phase separation for polymer synthesis.[31–37] PISA involves a solvophilic macroinitiator being chain-extended with a soluble monomer that polymerizes to form a solvophobic polymer. Self-assembly of the nascent block copolymers occurs when the extending block reaches a critical degree of polymerization (DP) such that it becomes sufficiently solvophobic to self-assemble.[34,38] *In situ* formation of polymeric nanoparticles, as opposed to molecularly dissolved block copolymers, keeps the reaction medium from becoming viscous during the polymerization.[39,40] However, despite the utility of PISA as a technique for nanoparticle preparation, the controlled synthesis of UHMW polymers has remained relatively unexplored using this route.[35] Recently, Armes and coworkers have reported on low-viscosity syntheses of high-molecular-weight hydrophilic block copolymers *via* PISA.[41–44] Polymeric nanoparticles were obtained by chain-extending hydrophilic macro-chain transfer agents with

George & Josephine Butler Polymer Research Laboratory, Center for Macromolecular Science & Engineering, Department of Chemistry, University of Florida, PO Box 117200, Gainesville, Florida 32611, USA. E-mail: sumerlin@chem.ufl.edu

† Electronic supplementary information (ESI) available. See DOI: https://doi.org/10.1039/d5sc00589b

Open Access Article. Published on 27 February 2025. Downloaded on 4/4/2026 1:24:43 AM. This article is licensed under a Creative Commons Attribution-NonCommercial 3.0 Unported Licence.

Open Access Article. Published on 27 February 2025. Downloaded on 4/4/2026 1:24:43 AM.
This article is licensed under a Creative Commons Attribution-NonCommercial 3.0 Unported Licence.

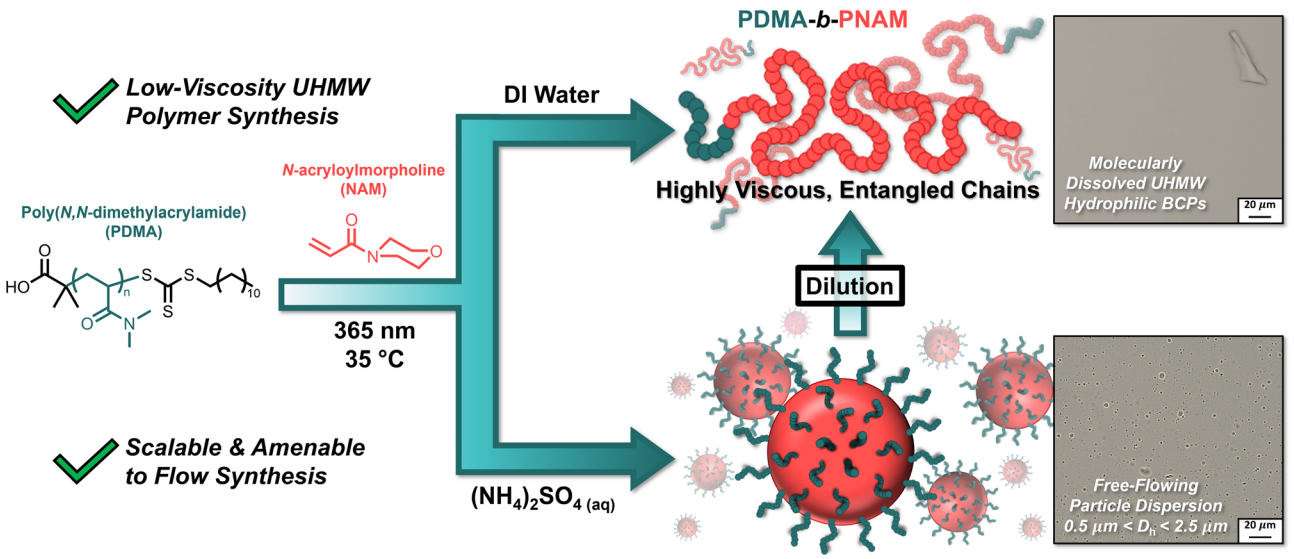

Fig. 1 Synthesis of hydrophilic ultra-high molecular weight (UHMW) polymers can be simplified by leveraging the benefits of dispersion polymerizations. The polymerization-induced self-assembly (PISA) of salt-sensitive poly(*N*-acryloylmorpholine) (PNAM) chains in aqueous $(NH_4)_2SO_4$ yields a free-flowing solution of UHMW polymer particles. Upon dilution with water, the $(NH_4)_2SO_4$ concentration is lowered sufficiently to solubilize the PNAM chains, resulting in a highly viscous solution of molecularly dissolved UHMW block copolymers.

monomers that yielded thermoresponsive core-forming blocks. Carrying out PISA in the presence of aqueous salt solutions caused the otherwise hydrophilic core-forming blocks to become hydrophobic as they grew, ultimately leading to self-assembly. This approach was able to access high molecular weight (M_n > 500 kg mol^{-1}, 1.9 < $Đ$ < 2.4) double-hydrophilic block copolymers (DHBCs) while maintaining a relatively low solution viscosity. However, the high amounts of exogenous initiator used resulted in many chains becoming permanently terminated, limiting the achievable molecular weights and resulting in polymers with relatively high dispersity.

We sought to combine these findings with our approach of leveraging PISA to simplify complex polymer synthesis[45] to prepare hydrophilic narrow-dispersity UHMW polymers *via* photoiniferter PISA. By chain-extending poly(*N*,*N*-dimethylacrylamide) (PDMA) macroiniferters with *N*-acryloylmorpholine (NAM) in aqueous $(NH_4)_2SO_4$, the nascent, salt-sensitive PNAM segments self-assembled into polymeric particles with eventual hydrodynamic diameters (D_h) of 500 nm–2.5 μm (Fig. 1). By using photoiniferter polymerization, we were able to reach molecular weights in excess of 10^6 g mol^{-1} without sacrificing dispersities. Dilution of the resultant particle solutions with water lowered the salt concentration, solubilizing the PNAM blocks and yielding a viscous solution of molecularly dissolved UHMW block copolymers. These results suggest PISA can be exploited as a tool to afford UHMW copolymers at high concentrations while avoiding the complication of high viscosity.

Results and discussion

We first set out to synthesize three PDMA macroiniferters of varying molecular weights to assess the necessary coronal chain size for steric stabilization of UHMW polymer core chains. UV

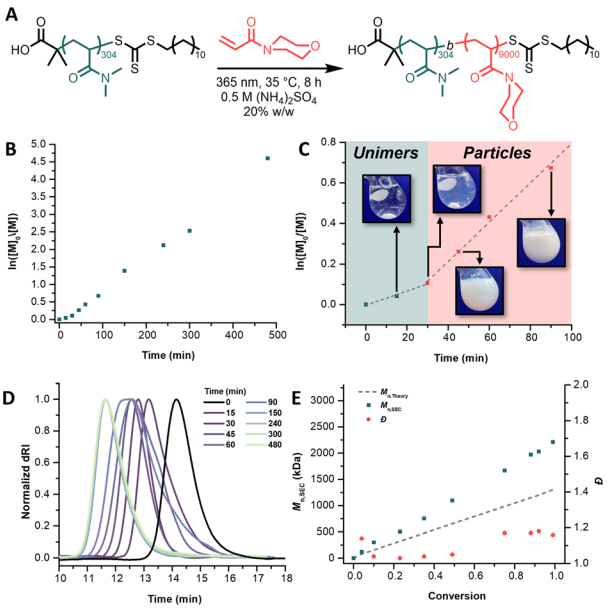

Fig. 2 (A) Reaction scheme depicting chain extension of poly(*N*,*N*-dimethylacrylamide) (PDMA) with *N*-acryloylmorpholine (NAM) in 0.5 M $(NH_4)_2SO_4$ *via* UV light-mediated photoiniferter polymerization; (B) pseudo-first-order kinetic plot of PDMA-*b*-PNAM particle synthesis (target core degree of polymerization = 9000) displaying a constant radical concentration during the polymerization; (C) increase in apparent polymerization rate before (green region, $k_{p,app}$ = 0.00351 min^{-1}) and after (red region, $k_{p,app}$ = 0.00969 min^{-1}) assembly, along with images of the nascent polymer particles corresponding to 15, 30, 45, and 90 min (left to right); (D) size-exclusion chromatograms showing molecular weight evolution during PISA as indicated by peaks shifting to lower elution times; (E) close agreement between theoretical (gray dashed line) and experimental (green squares) molecular weights and low dispersities (red squares) indicating good control for the duration of the polymerization.

© 2025 The Author(s). Published by the Royal Society of Chemistry

Open Access Article. Published on 27 February 2025. Downloaded on 4/4/2026 1:24:43 AM. This article is licensed under a Creative Commons Attribution-NonCommercial 3.0 Unported Licence.

Table 1 Photoiniferter polymerization-induced self-assembly (PISA) conditions[a]

Macroiniferter	Target core DP	$M_{n,Theory}$ (kg mol^{-1})[b]	$M_{n,SEC}$ (kg mol^{-1})[c]	$Đ$[c]
MI_{30k} (no $(NH_4)_2SO_4$)	9000	1300	1780	1.23
MI_{30k}	9000	1300	2550	1.19
	12 000	1720	2550	1.17
MI_{80k}	9000	1350	1760	1.19
	12 000	1780	2420	1.13
	14 000	2060	1970	1.21
	16 000	2340	2410	1.21
MI_{120k}	9000	1390	1680	1.27
	12 000	1820	1880	1.21
	14 000	2100	1970	1.23
	16 000	2380	2560	1.15
	18 000	2670	2080	1.11

[a] All chain extensions conducted in 0.5 M $(NH_4)_2SO_4$ unless otherwise noted. [b] Calculated from the conversion of monomer determined by ^{1}H NMR spectroscopy. [c] Determined by size-exclusion chromatography (SEC) equipped with a multiangle light-scattering detector.

light-mediated photoiniferter polymerization (365 nm, 3.5 mW cm^{-2}) afforded PDMA macroiniferters of 30.5 kg mol^{-1} (MI_{30k}), 81.4 kg mol^{-1} (MI_{80k}), and 124.1 kg mol^{-1} (MI_{120k}).[46] Size-exclusion chromatography (SEC) analysis indicated well-controlled polymerizations with close agreement between theoretical and experimental molecular weights and low dispersities (Table S1†). With macroiniferters in hand, we then began conducting PISA experiments to find the upper limit of the number-average degree of polymerization (DP) for the core block that each macroiniferter could stabilize before macroscopic precipitation of the polymer chains was observed. Informed by recent findings by Armes and coworkers, we chose to chain extend our macroiniferters with *N*-acryloylmorpholine (NAM) in 0.5 M $(NH_4)_2SO_4$ (Fig. 2A).[41,42]

To overcome the high extents of irreversible chain termination that had been previously observed, we chose to perform our PISA reactions *via* photoiniferter polymerization. This approach resulted in drastically increased chain-end fidelity, which consequently afforded access to UHMW PDMA-*b*-PNAM with excellent control over molecular weight distributions ($Đ$ < 1.3) (Fig. 2). Linear pseudo-first-order kinetics were observed for the chain extension of MI_{30k} with a target core DP of 9000 (Fig. 2B). Closer inspection revealed a marked increase in the apparent rate constant of propagation ($k_{p,app}$) after 30 min, coinciding with when self-assembly was visually observed (Fig. 2C). A transition from a completely transparent, homogeneous solution to a slightly blue, turbid, heterogeneous one was a result of the PDMA-*b*-PNAM particles nucleating and scattering light.[47–49] SEC analysis (Fig. 2D) showed shifts to lower elution times as the PDMA macroiniferter was chain extended with NAM, implying efficient chain extensions with high maintenance of chain-end fidelity. SEC kinetic analysis also indicated close agreement between theoretical and experimental molecular weights while maintaining low dispersities (Fig. 2E).

We then expanded our macroiniferter and target core DP scope. These experiments are summarized in Table 1. The concentration of $(NH_4)_2SO_4$ and solids content were held at 0.5 M and 20% w/w, respectively, for all reactions. Chain

Table 2 *Z*-Average hydrodynamic diameters (D_z) and polydispersity indices (PDI) determined by dynamic light scattering[a]

Macroiniferter	Target core DP	D_z (nm)	PDI
MI_{30k}	9000	2165	0.002
	12 000	Sed.	Sed.
MI_{80k}	9000	569	0.009
	12 000	835	0.204
	14 000	873	0.053
	16 000	1036	0.185
MI_{120k}	9000	527	0.034
	12 000	752	0.186
	14 000	683	0.022
	16 000	727	0.017
	18 000	1278	0.076

[a] 0.1% w/w of particles in 0.5 M $(NH_4)_2SO_4$.

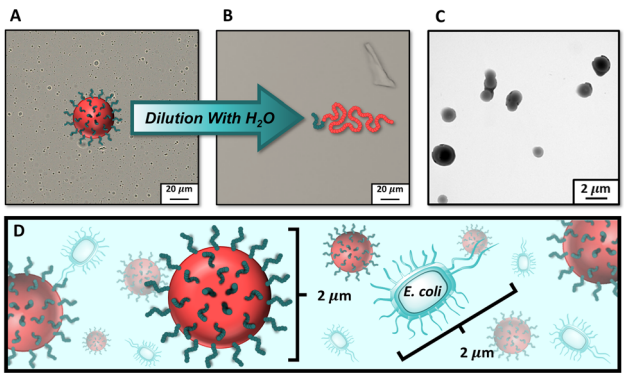

Fig. 3 (A) Visible light microscopy (VLM) image of PDMA-*b*-PNAM particles made by chain extending MI_{30k} with 9000 equiv. of NAM ($PDMA_{304}$-*b*-$PNAM_{9000}$); (B) VLM image of $PDMA_{304}$-*b*-$PNAM_{9000}$ particles after a 1 : 1 dilution with water, showing the complete dissociation of the particles into molecularly dissolved chains invisible by VLM; (C) transmission electron micrograph of $PDMA_{304}$-*b*-$PNAM_{9000}$ particles; (D) cartoon comparing the size of the $PDMA_{304}$-*b*-$PNAM_{9000}$ particles to that of *Escherichia coli* cells.

Open Access Article. Published on 27 February 2025. Downloaded on 4/4/2026 1:24:43 AM. This article is licensed under a Creative Commons Attribution-NonCommercial 3.0 Unported Licence.

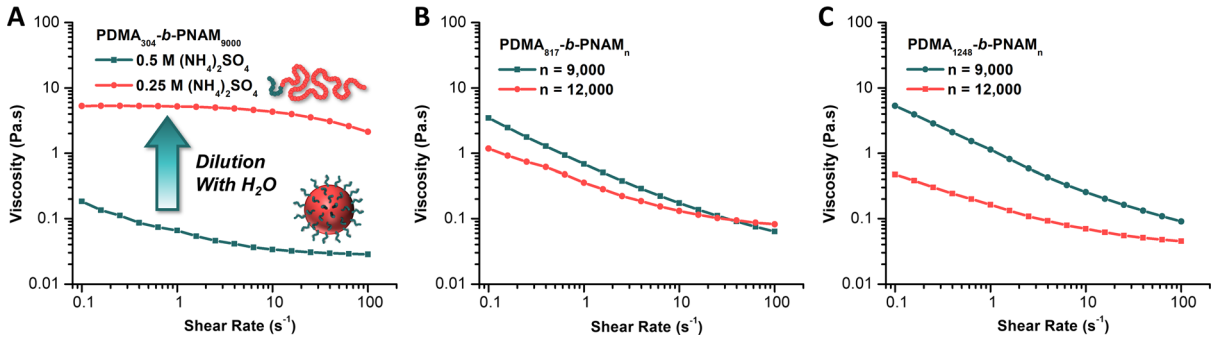

Fig. 4 Oscillatory rheology data of: (A) $PDMA_{304}$-*b*-$PNAM_{9000}$ as particles in the native 0.5 M $(NH_4)_2SO_4$ solution (green) and as molecularly dissolved chains after a 1 : 1 dilution of the native solution with pure water (red), (B) MI_{80k} after chain extension with 9000 (green) and 12 000 (red) equivalents of NAM, and (C) MI_{120k} after chain extension with 9000 (green) and 12 000 (red) equivalents of NAM, both in a 0.5 M $(NH_4)_2SO_4$ solution.

extending MI_{30k} with 9000 equiv. of NAM in 0.25 M $(NH_4)_2SO_4$ resulted in a physically entangled, turbid gel. In 1.0 M $(NH_4)_2SO_2$, the same polymerization conditions resulted in sedimentation of polymer product in under 1 h. Upon chain extending MI_{30k} with a target core DP of 12 000, sedimentation was again observed. MI_{80k} and MI_{120k}, however, were large enough to stabilize PNAM DPs up to 16 000 and 18 000, respectively, resulting in the desired free-flowing dispersions of polymer particles. These results highlight the importance of selecting an MI of sufficient length to stabilize growth of UHMW salt-responsive segments.

Resultant polymer particles were then characterized by dynamic light scattering (DLS) (Table 2). Interestingly, we observed that chain extending MI_{30k} with 9000 equiv. of NAM resulted in polymer particles with *Z*-average hydrodynamic diameters (D_z) much larger than the rest of the formulations, despite it involving the lowest molecular weight macroiniferter and lowest core chain DP. The large size of these particles ($D_z > 2$ μm, Fig. S16†) permitted the use of visible light microscopy (VLM) for particle imaging (Fig. 3A). By VLM, we observed distinct spherical morphologies with sizes similar to those measured by DLS (Table 2). Upon dilution with water, the particles completely dissociated into molecularly dissolved chains invisible by VLM (Fig. 3B). To further investigate the structure of the $PDMA_{304}$-*b*-$PNAM_{9000}$ particles, we relied on transmission electron microscopy (TEM) (Fig. 3C). The resulting TEM images corroborated our observations by VLM, showing large particles with spherical morphologies.

We then employed oscillatory rheology to study the viscosity of the particle dispersions. We observed a decrease in solution viscosity with increasing shear rate, indicative of shear-thinning behaviors (Fig. 4). Furthermore, we compared the viscosity of the native $PDMA_{304}$-*b*-$PNAM_{9000}$ particle solution (0.5 M $(NH_4)_2SO_4$) to that of a 1 : 1 dilution of the same solution with DI water (0.25 M $(NH_4)_2SO_4$). Upon dilution, the completely opaque, white solution of particles becomes perfectly clear and homogeneous with an accompanying drastic increase in observed viscosity. This observation is consistent with dilution of the salt below the level needed to induce insolubility of the PNAM block. Once the core block becomes solvophilic, the block copolymer aggregates are disassembled to yield molecularly dissolved unimers. This occurrence leads to a counterintuitive increase in viscosity upon dilution.[41,42]

Rheological analysis gave viscosities of 0.185 Pa·s and 5.30 Pa·s for the native and diluted solution, respectively, at a shear rate of 0.1 s^{-1}. At a shear rate of 100 s^{-1}, these became 0.0283 Pa·s and 2.13 Pa·s for the native and diluted solutions, respectively, a difference of approximately two orders of magnitude (Fig. 4A). Further analysis of particle solutions made from chain extending MI_{80k} (Fig. 4B) and MI_{120k} (Fig. 4C) with 9000 and 12 000 equiv. of NAM revealed similarly low viscosities for the respective native particle solutions. We observed that the solution viscosities were higher for particles of smaller D_z, which we reasoned was due to the higher surface area of the smaller particles resulting in more significant interparticle interactions.[50] We also observed that for a given macroiniferter the viscosity decreased significantly when the core DP increased from 9000 to 12 000 (MI_{80k}, Fig. 4B; MI_{120k}, Fig. 4C). While, outwardly, this may seem counterintuitive, we used the same rationale as before, such that larger particles (those with core DP = 12 000) result in lower solution viscosities than the dispersions of smaller particles (those with core DP = 9000). Nonetheless, the low viscosities of all particle solutions measured relative to the diluted, molecularly dissolved polymer solution indicated the amenability of these reactions to continuous flow synthesis, a primary focus of ongoing research in our group.

Conclusions

Here, we report on the successful heterogeneous synthesis of UHMW hydrophilic polymers by photoiniferter PISA. By exploiting PISA, we developed a novel method towards UHMW polymer synthesis, wherein the viscosities of these concentrated, but free-flowing, PDMA-*b*-PNAM particle dispersions were kept relatively low. These results demonstrate a simple, tuneable method by which one can synthesize hydrophilic UHMW polymers in dispersed media by leveraging both the inherent low viscosities of polymer particle dispersions and the salt-dependent hydrophilicity of water-soluble polymers. These

© 2025 The Author(s). Published by the Royal Society of Chemistry

Open Access Article. Published on 27 February 2025. Downloaded on 4/4/2026 1:24:43 AM. This article is licensed under a Creative Commons Attribution-NonCommercial 3.0 Unported Licence.

findings have the potential to make industrial-scale syntheses of hydrophilic UHMW polymers more facile and feasible, with the hope of bringing these unique materials to commercial prominence.

Data availability

The data supporting this article have been included as part of the ESI.†

Author contributions

Conceptualization, C. B. E., K. C. S., B. S. S.; methodology, C. B. E., K. C. S., D. E. C., M. K. V., B. S. S.; investigation, C. B. E., K. C. S., D. E. C., M. K. V., M. E. L.; data curation, C. B. E., K. C. S., D. E. C., M. K. V.; writing, C. B. E., J. I. B., B. S. S.; supervision, B. S. S.; project administration, B. S. S.; funding acquisition, B. S. S.

Conflicts of interest

There are no conflicts to declare.

Acknowledgements

We gratefully acknowledge Professor Steven P. Armes for helpful discussion and Justin Ellenburg for obtaining visible light microscopy images for this publication. M. E. L. was supported by the Department of Defense (DoD) through the National Defense Science & Engineering Graduate (NDSEG) Fellowship Program. This material is based on work supported by the National Science Foundation (DMR-2404144) and the DoD through the ARO (W911NF2410050, W911NF2310260).

References

1 M. Streicher, V. Boyko and A. Blanazs, *ACS Appl. Mater. Interfaces*, 2023, **15**, 59054.
2 Y. Kamiyama, R. Tamate, T. Hiroi, S. Samitsu, K. Fujii and T. Ueki, *Sci. Adv.*, 2022, **8**, eadd0226.
3 J. K. D. Mapas, T. Thomay, A. N. Cartwright, J. Ilavsky and J. Rzayev, *Macromolecules*, 2016, **49**, 3733–3738.
4 Y. Kamiyama, R. Tamate, K. Fujii and T. Ueki, *Soft Matter*, 2022, **18**, 8582–8590.
5 R. N. Carmean, T. E. Becker, M. B. Sims and B. S. Sumerlin, *Chem*, 2017, **2**, 93–101.
6 R. N. Carmean, M. B. Sims, C. A. Figg, P. J. Hurst, J. P. Patterson and B. S. Sumerlin, *ACS Macro Lett.*, 2020, **9**, 613–618.
7 J. Rzayev and J. Penelle, *Angew. Chem., Int. Ed.*, 2004, **43**, 1691–1694.
8 R. W. Simms and M. F. Cunningham, *Macromolecules*, 2007, **40**, 860–866.
9 L. Mueller, W. Jakubowski, K. Matyjaszewski, J. Pietrasik, P. Kwiatkowski, W. Chaladaj and J. Jurczak, *Eur. Polym. J.*, 2011, **47**, 730–734.
10 P. Zhang, Q. Xu, W. Mao, J. Lv, H. Tang and H. Tang, *Polymers*, 2023, **15**, 2501.
11 M. Yuan, L. Xu, X. Cui, J. Lv, P. Zhang and H. Tang, *Polymers*, 2020, **12**, 2747.
12 S. K. De and M. Bhattacharjee, *J. Polym. Sci., Part A:Polym. Chem.*, 2013, **51**, 1540–1549.
13 V. Percec, T. Guliashvili, J. S. Ladislaw, A. Wistrand, A. Stjerndahl, M. J. Sienkowska, M. J. Monteiro and S. Sahoo, *J. Am. Chem. Soc.*, 2006, **128**, 14156–14165.
14 A. Reyhani, S. Allison-Logan, H. Ranji-Burachaloo, T. G. McKenzie, G. Bryant and G. G. Qiao, *J. Polym. Sci., Part A: Polym. Chem.*, 2019, **57**, 1922–1930.
15 R. Li, S. Zhang, Q. Li, G. G. Qiao and Z. An, *Angew. Chem., Int. Ed.*, 2022, **61**, e202213396.
16 Y. T. Chou, W. R. Lee and S. S. Yu, *Macromolecules*, 2024, **57**, 9241–9249.
17 Z. An, *ACS Macro Lett.*, 2020, **9**, 350–357.
18 Y. Lee, C. Boyer and M. S. Kwon, *Chem. Soc. Rev.*, 2023, **52**, 3035–3097.
19 R. Li and Z. An, *Angew. Chem., Int. Ed.*, 2020, **59**, 22258–22264.
20 E. K. Stacy, M. L. McCormick, K. C. Stevens, P. E. Jankowski, J. Aguinaga, D. L. Patton, B. S. Sumerlin and T. D. Clemons, *ACS Macro Lett.*, 2024, **13**, 1662–1669.
21 R. W. Hughes, M. E. Lott, R. A. S. Olson and B. S. Sumerlin, *Prog. Polym. Sci.*, 2024, **156**, 101871.
22 J. B. Young, S. L. Goodrich, J. A. Lovely, M. E. Ross, J. I. Bowman, R. W. Hughes and B. S. Sumerlin, *Angew. Chem., Int. Ed.*, 2024, **63**, e202408592.
23 L. Trachsel, K. A. Stewart, D. Konar, J. D. Hillman, J. A. Moerschel and B. S. Sumerlin, *J. Am. Chem. Soc.*, 2024, **146**, 16257–16267.
24 L. Trachsel, D. Konar, J. D. Hillman, C. L. G. Davidson and B. S. Sumerlin, *J. Am. Chem. Soc.*, 2024, **146**, 1627–1634.
25 R. W. Hughes, M. E. Lott, I. S. Zastrow, J. B. Young, T. Maity and B. S. Sumerlin, *J. Am. Chem. Soc.*, 2024, **146**, 6217–6224.
26 L. E. Diodati, A. J. Wong, M. E. Lott, A. G. Carter and B. S. Sumerlin, *ACS Appl. Polym. Mater.*, 2023, **5**, 9714–9720.
27 A. C. Lehnen, J. A. M. Kurki and M. Hartlieb, *Polym. Chem.*, 2022, **13**, 1537.
28 R. A. Olson, M. E. Lott, J. B. Garrison, C. L. G. Davidson, L. Trachsel, D. I. Pedro, W. G. Sawyer and B. S. Sumerlin, *Macromolecules*, 2022, **55**, 8451–8460.
29 C. G. L. Davidson, M. E. Lott, L. Trachsel, A. J. Wong, R. A. Olson, D. I. Pedro, W. G. Sawyer and B. S. Sumerlin, *ACS Macro Lett.*, 2023, **12**, 1224–1230.
30 M. E. Lott, L. Trachsel, E. Schué, C. L. G. Davidson, R. A. Olson S, D. I. Pedro, F. Chang, Y. Hong, W. G. Sawyer and B. S. Sumerlin, *Macromolecules*, 2024, **57**, 4007–4015.
31 D. J. Rucco, B. E. Barnes, J. B. Garrison, B. S. Sumerlin and D. A. Savin, *Biomacromolecules*, 2020, **21**, 5077–5085.
32 A. B. Korpusik, Y. Tan, J. B. Garrison, W. Tan and B. S. Sumerlin, *Macromolecules*, 2021, **54**, 354–7363.
33 J. Y. Rho, G. M. Scheutz, S. Häkkinen, J. B. Garrison, Q. Song, J. Yang, R. Richardson, S. Perrier and B. S. Sumerlin, *Polym. Chem.*, 2021, **12**, 3947–3952.
34 N. J. W. Penfold, J. Yeow, C. Boyer and S. P. Armes, *ACS Macro Lett.*, 2024, **8**, 1029–1054.

© 2025 The Author(s). Published by the Royal Society of Chemistry

Open Access Article. Published on 27 February 2025. Downloaded on 4/4/2026 1:24:43 AM.
This article is licensed under a Creative Commons Attribution-NonCommercial 3.0 Unported Licence.

35 H. Wang, Y. Huang, J. Y. Rho, A. B. Korpusik, M. Hoteit, J. B. Garrison and B. S. Sumerlin, *Polym. Chem.*, 2024, **8**, 5255–5446.
36 N. J. Warren and S. P. Armes, *J. Am. Chem. Soc.*, 2014, **136**, 10174–10185.
37 A. J. Wong, C. B. Eades, J. I. Bowman, C. L. G. Davidson IV and B. S. Sumerlin, *Polym. Chem.*, 2025, **16**, 620–625.
38 C. A. Figg, A. Simula, K. A. Gebre, B. S. Tucker, D. M. Haddleton and B. S. Sumerlin, *Chem. Sci.*, 2015, **6**, 1230–1236.
39 L. P. D. Ratcliffe, M. J. Derry, A. Ianiro, R. Tuinier and S. P. Armes, *Angew. Chem., Int. Ed.*, 2019, **58**, 18964–18970.
40 S. L. Canning, G. N. Smith and S. P. Armes, *Macromolecules*, 2016, **49**, 1985–2001.
41 R. J. McBride, J. F. Miller, A. Blanazs, H. J. Hähnle and S. P. Armes, *Macromolecules*, 2022, **55**, 7380–7391.
42 R. J. McBride, E. Geneste, A. Xie, A. J. Ryan, J. F. Miller, A. Blanazs, C. Rösch and S. P. Armes, *Macromolecules*, 2024, **57**, 2432–2445.
43 V. J. Cunningham, M. J. Derry, L. A. Fielding, O. M. Musa and S. P. Armes, *Macromolecules*, 2016, **49**, 4520–4533.
44 C. György, J. S. Wagstaff, S. J. Hunter, E. U. Etim and S. P. Armes, *Macromolecules*, 2024, **57**, 6816–6827.
45 G. M. Scheutz, J. I. Bowman, S. Mondal, J. Y. Rho, J. B. Garrison, J. Korpanty, N. C. Gianneschi and B. S. Sumerlin, *ACS Macro Lett.*, 2023, **12**, 454–461.
46 R. W. Hughes, M. E. Lott, J. I. Bowman and B. S. Sumerlin, *ACS Macro Lett.*, 2023, **12**, 14–19.
47 A. Blanazs, J. Madsen, G. Battaglia, A. J. Ryan and S. P. Armes, *J. Am. Chem. Soc.*, 2011, **133**, 16581–16587.
48 B. Couturaud, P. G. Georgiou, S. Varlas, J. R. Jones, M. C. Arno, J. C. Foster and R. K. O'Reilly, *Macromol. Rapid Commun.*, 2019, **40**, 1800460.
49 J. I. Bowman, C. B. Eades, M. A. Vratsanos, N. C. Gianneschi and B. S. Sumerlin, *Angew. Chem., Int. Ed.*, 2023, **62**, e202309951.
50 M. Rubinstein and R. H. Colby, *Polymer Physics*, Oxford University Press, Oxford, England, 2003.

© 2025 The Author(s). Published by the Royal Society of Chemistry